

# Combined and targeted drugs delivery system for colorectal cancer treatment: Conatumumab decorated, reactive oxygen species sensitive irinotecan prodrug and quercetin co-loaded nanostructured lipid carriers

Youqiang Liu<sup>a\*</sup>, Hongxin Zhang<sup>b\*</sup>, Haijing Cui<sup>c</sup>, Futong Zhang<sup>b</sup>, Liyan Zhao<sup>d</sup>, Yibing Liu<sup>e</sup> and Qingju Meng<sup>f</sup>

<sup>a</sup>The Second Department of General Surgery, the Fourth Hospital of Hebei Medical University, Hebei Cancer Hospital, Shijiazhuang, Hebei Province, China; <sup>b</sup>Ward 1 of Department of Oncology, Shijiazhuang People's Hospital, Shijiazhuang, Hebei Province, China; <sup>c</sup>Ward 2 of Department of Oncology, Shijiazhuang People's Hospital, Shijiazhuang, Hebei Province, China; <sup>d</sup>Department of Endocrinology, the First Hospital of Xingtai, Xingtai, Hebei Province, China; <sup>e</sup>Department of Medical Oncology, the Fourth Hospital of Hebei Medical University, Hebei Cancer Hospital, Shijiazhuang, Hebei Province, China; <sup>f</sup>Department of Osteology, the First Hospital of Xingtai, Xingtai, Hebei Province, China

## ABSTRACT

**Purpose:** Colorectal cancer (CRC) is the third most frequently diagnosed cancer and this study aimed to develop a conatumumab decorated, irinotecan prodrug and quercetin co-loaded delivery system for combined and targeted colorectal cancer treatment.

**Methods:** A conatumumab (C) decorated, irinotecan prodrug (I-p) and quercetin (Q) co-encapsulated NLC (C I-p/Q NLC) was developed. *In vitro* and *in vivo* antitumor efficiency of NLC was evaluated on CRC cells and mice xenograft.

**Results:** The results showed that the HT-29 cells uptake of C I-p/Q NLC was over 70%. Reactive oxygen species (ROS) sensitive irinotecan prodrug formulation showed improved drug release ability in hypoxic conditions. C I-p/Q NLC showed significantly higher cytotoxicity than non-decorated NLC, single drug-loaded NLC and free drugs. *In vivo* studies in a CRC-bearing model corroborated the capability of nanoparticles for the inhibition of cancer, leading to a reduction of tumor growth without systemic toxicity.

**Conclusion:** The conatumumab decorated, ROS sensitive prodrug contained combination nano-system is a promising platform for CRC therapy.

## ARTICLE HISTORY

Received 10 November 2021  
Revised 3 January 2022  
Accepted 3 January 2022

## KEYWORDS





Colorectal cancer; irinotecan prodrug; lipid nanoparticles; reactive oxygen species sensitive

## Introduction

Colorectal cancer (CRC) is the third most frequently diagnosed cancer and the fourth leading cause of cancer-related death in the world, and its development is estimated to be over 2.2 million new incidents and 1.1 million deaths in 2030 globally (Arnold et al., 2017). Approximately 50–60% of patients diagnosed with colorectal cancer will develop colorectal metastases, and most of them have an unresectable disease (Alberts et al., 2005; European Colorectal Metastases Treatment Group, 2006). Chemotherapy remains the primary treatment regimen for metastatic CRC (mCRC) patients (Masi et al., 2008; Lucas et al., 2011). The first-line therapy options for advanced or metastatic CRC include FOLFIRI (leucovorin, 5-fluorouracil, oxaliplatin and irinotecan) and FOLFOX (leucovorin, 5-fluorouracil, oxaliplatin). Several phase III trials have strongly proven that the FOLFOXIRI regimen, compared with FOLFIRI, improves RR (response rate), PFS (progression-free survival), and OS (overall survival) for mCRC patients, and

with increased and manageable toxicity for lack of targeting ability (Falcone et al., 2007; Masi et al., 2008). Therefore, there is a critical need for strategies to deliver therapeutic agents to metastatic cancer, thus improving efficacy and reducing toxicity. Tumor necrosis factor-related apoptosis-inducing ligand (TRAIL) could induce apoptosis upon binding to its death domain-containing receptors, TRAIL receptor (DR5) (Bavi et al., 2010). Expression of TRAIL receptors is higher in CRC compare with normal colorectal mucosa and targeted therapy with TRAIL leads to preferential killing of tumor cells sparing normal cells. Conatumumab (AMG 655) is a fully human therapeutic antibody that has been developed to bind the extracellular domain of DR5, which is now currently in clinical trials as a single agent or in combination chemotherapies for the treatment of pancreatic and colorectal cancers (Tiernan et al., 2013).

Irinotecan (I), a water-soluble prodrug of SN38 (7-ethyl-10-camptothecin), its property of lower transforming ratio to the active metabolite (only 2–8 percent) makes researchers

**CONTACT:** Yibing Liu  [lyb.he@163.com](mailto:lyb.he@163.com)  Department of Medical Oncology, the Fourth Hospital of Hebei Medical University, Hebei Cancer Hospital, Shijiazhuang, Hebei Province, 050010, China; Qingju Meng  [qingjumeng@163.com](mailto:qingjumeng@163.com)  Department of Osteology, the First Hospital of Xingtai, Xingtai, Hebei Province, 054001, China

\*Youqiang Liu and Hongxin Zhang are the co-first authors, who contributed equally to this work.

© 2022 The Author(s). Published by Informa UK Limited, trading as Taylor & Francis Group.

This is an Open Access article distributed under the terms of the Creative Commons Attribution-NonCommercial License (<http://creativecommons.org/licenses/by-nc/4.0/>), which permits unrestricted non-commercial use, distribution, and reproduction in any medium, provided the original work is properly cited.

devoted themselves to novel strategies for improving its therapeutic effect (Slatter et al., 1997; Mathijssen et al., 2001). Those strategies include prodrug technology and nanocarriers (Wang et al., 2013; Whang et al., 2018; Xing et al., 2019). Herein, based on present studies, further CRC tumor-targeted lipid nanoparticles were engineered by combining lipid prodrug strategy, reactive oxygen species (ROS) sensitive technology and lipid carriers. In our designed prodrug, a ROS sensitive linker (thioetheral group, TK) is directly conjugated to the phenolic hydroxyl group (C<sub>10</sub>-OH) of SN-38 and the carboxyl group of stearic acid (SA): 1) SA group, anticipating to obtain the lipophilic conjugate of SN-38 for enhancing the drug loading in lipid nanoparticles, the possibility of stabilization of the active lactone form and the cell membrane penetration capacity; 2) TK linker, tumor-specific accumulation because of higher levels of ROS in cancer cells than that in comparison with normal, then burst release of SN-38 (Fang et al., 2016; Xing et al., 2019).

Quercetin (Q) is a type of widespread natural bioflavonoid compound that originates from multifarious edible fruits, vegetables, seeds, and tea (Xu et al., 2015). The anticancer effects of quercetin have been reported in several cancers, including colorectal cancer (Zhang et al., 2019). A combination of quercetin with other drug has been developed by researchers for tumor therapy (Lv et al., 2016; Liu et al., 2017; Zhang et al., 2019). However, the properties of quercetin are limited due to low bioavailability, low solubility in water, rapid clearance from the body, fast metabolism, and degradation by enzymes (Yarjanli et al., 2019). Therefore, suitable drug delivery systems are needed.

Lipid nanoparticles are an interesting parenteral delivery system for poorly water-soluble drugs (Roese & Bunjes, 2017). Nanostructured lipid carriers (NLC) are composed of a binary mixture of solid lipid and a spatially different liquid lipid as the carrier (Zhang et al., 2016). NLC has been used for the co-delivery of drugs for cancer therapy (Zhang et al., 2018). In this study, a conatumumab (C) irinotecan prodrug (I-p) and quercetin co-encapsulated NLC (C I-p/Q NLC) was constructed and used for the targeted therapy of CRC. *In vitro* and *in vivo* antitumor efficiency of NLC was evaluated on CRC cells and mice xenograft.

## Materials and methods

### Materials and animals

Stearic acid (SA), glycerin monostearate (GMS), Soybean oil (SO), soybean lecithin (SL), fetal bovine serum (FBS), 3-(4,5)-dimethylthiazolium-2-yl-3,5-diphenyltetrazolium bromide (MTT), propidium iodide (PI) and coumarin-6 (Cou-6) were purchased from Sigma-Aldrich (St. Louis, MO, USA). Irinotecan (I, purity  $\geq 98.5\%$ ) and Quercetin (Q, purity  $\geq 95\%$ ) was purchased from Aikon Biopharmaceutical R&D Co., Ltd. (Nanjing, China). HT-29 cells and human normal colonic epithelial cells (NCM460 cells) were obtained from American Type Culture Collection (Manassas, VA). BALB/c nude mice (6–8 weeks) were purchased from Beijing Vital River Laboratory Animal Technology Co., Ltd (Beijing, China) and CRC xenograft mice

were generated by injecting HT-29 cells ( $1 \times 10^7$  each) subcutaneously into the abdominal cavity of mice. The animal experiments have followed the guidance of the National Institutes of Health (NIH) for the care and use of laboratory animals Publications and approved by the Animal Care and Use Committee of Hebei the Fourth Hospital of Hebei Medical University (No. IACUC-4th Hos Hebmu-2021016).

### Synthesize of an irinotecan prodrug

An irinotecan prodrug (I-p) was synthesized by conjugating the phenolic hydroxyl group of irinotecan with the carboxyl group of SA through a ROS-sensitive thioetheral cross-linker (Figure 1(A)) (Ling et al., 2015). TK linker, EDC-HCl, NHS, and DMAP were dissolved in acetonitrile. SN-38 was added to acetonitrile solution and stirred for 10 h to get I-TK. Next, SA was dissolved in acetonitrile along with EDC-HCl and NHS, stirred for 2 h, followed by adding I-TK into the SA mixture and stirred for another 12 h. The final crude product was filtered, concentrated under vacuum, purified by column chromatography on silica gel using dichloromethane/methanol (10:1 v/v) as a mobile phase. The formation of I-p was characterized by LC-MS and <sup>1</sup>H NMR.

### Preparation of NLC

NLC was prepared by the hot melting high-pressure homogenization method (Yang et al., 2019). Briefly, solid lipid (GMS, 100 mg) and liquid lipid (SO, 100 mg) were mixed together and melted at 65 °C (oil phase). SL (50 mg) and Tween 80 (0.5% w/v) were dispersed in double-distilled water heated to 65 °C (aqueous phase). Then the aqueous phase was mixed with the oil phase under high-speed shearing (10,000 rpm) to prepare pre-emulsion. Next, the pre-emulsion was then immediately passed through a high-pressure homogenizer (5 cycles at 50 MPa). The blank NLC was obtained by solidification in an ice bath.

Irinotecan prodrug (I-p) and quercetin co-encapsulated NLC (I-p/Q NLC) was prepared by the same method by adding additional I-p (20 mg) and Q (20 mg) into the oil phase. Single I-p, irinotecan or quercetin-loaded NLC was prepared by the same method by adding additional I-p (40 mg), I (40 mg), or Q (40 mg) into the oil phase, named I-p NLC, I NLC and Q NLC. Free I and Q mixed solutions were prepared and named free I/Q.

C I-p/Q NLC was achieved by adding 20 mL of 0.1 M EDC and 200 mL of 0.7 M NHS to the I-p/Q NLC suspension, which was kept at room temperature for 1 h under moderate stirring. Then monoclonal antibody (conatumumab) solution (10 mL of 1 mg/mL) was added to and incubated at 4 °C overnight. Finally, solutions were centrifuged (20,000 g for 1 h) and resuspended in PBS to remove excess of non-conjugated antibodies. Antibody conjugation was quantified spectrophotometrically using a microBCA kit following the manufacturer's instructions.

### Characterization of NLC

The morphology of the C I-p/Q NLC was investigated by transmission electron microscopy (TEM) (Li et al., 2017; Zhu et al., 2017). A Zetasizer (Nano ZS90, Malvern Instruments Ltd., Malvern, UK) was used to determine the particle size, size distribution (PDI) and zeta potential of NLC.

Drug loading efficiency (LE) was calculated as the percentage ratio of the actual drugs loading of the particles to the total drugs applied to the composite NLC. Drugs loaded NLC was centrifugated (15,000 rpm, 10 min) to separate the unloaded drugs. The amount of Q was determined by UV-Vis spectrometry (at  $\lambda_{\text{max}}$  of 370 nm) (Rashedi et al., 2019). The amount of I was separated by a C18 column (200  $\times$  4.6 mm, 5  $\mu\text{m}$ ). The mobile phase consisted of acetonitrile and water (40/60, v/v) with a flow rate of 1.0 mL/min. The fluorescence detection was set at 370 nm (Wang et al., 2020).

### In vitro stability of NLC

The stability of NLC was demonstrated by monitoring the sizes in the presence of 50% fetal bovine serum (FBS) (Yuan et al., 2016). Briefly, various kinds of NLC were mixed with an equal volume of FBS under gentle shaking (100 rpm at 37  $^{\circ}\text{C}$ ) for 48 h. At predetermined time points, 200  $\mu\text{L}$  of the sample was taken out and diluted for the particle size measurements by a Zetasizer as described in the above section. The stability of NLC was also conducted without the presence of FBS.

### In vitro drug release from NLC

The amounts of drugs released from NLC were measured by the dialysis method in normoxia or hypoxic (created by adding 10 mM of glutathione) condition (Shao et al., 2015). Briefly, C I-p/Q NLC, I-p/Q NLC, I-p NLC, I NLC and Q NLC were placed in the dialysis bags containing PBS (pH 7.4) separately. Then, the bags were placed in the release medium (0.1% Tween 80 in PBS, pH 7.4) which were stirred at 100 rpm using a mini-stir bar. At predetermined time points, the release medium (200  $\mu\text{L}$ ) was collected and replaced with the same amount of fresh medium. The amounts of released drugs were determined by the method in the above "Characterization of NLC" section.

### Cellular uptake of NLC

Cellular uptake of NLC was evaluated using Cou-6 as the fluorescent probe (Ruan et al., 2018). Cou-6 contained NLC was prepared by adding Cou-6 (10 mg) into the oil phase. The HT-29 cells were seeded in 24-well culture plates (5  $\times$  10<sup>4</sup> cells per well) and incubated for 24 h. Then cells were incubated with different kinds of NLC for 1 h. After the incubation, Cells were washed three times with D-Hank's solution and photographed by fluorescence microscopy and analyzed using a flow cytometer.

### Synergistic cytotoxicity of drug combination in NLC

The cytotoxicity of NLC and free drugs against HT-29 cells or NCM460 cells was assessed using the MTT assay (Zhang et al., 2019). Cells were seeded in 96-well plates (5  $\times$  10<sup>3</sup> cells per well) and incubated for 24 h before treatment. Then the culture medium was withdrawn and a fresh medium containing NLC or free drugs at different concentrations were added to each well and incubated for 72 h. Cytotoxicity was determined by the MTT assay. The synergy of drugs on HT-29 cells was evaluated using the Chou and Talalay method to calculate the combination index (Chou & Talalay, 1984). CI was calculated by the equation:  $CI = (C_1)/(C_x)_1 + (C_2)/(C_x)_2$ , where (C)<sub>1</sub> and (C)<sub>2</sub> are the concentrations for a single drug after combination that inhibits x% of cell growth, and (C<sub>x</sub>)<sub>1</sub> and (C<sub>x</sub>)<sub>2</sub> are the concentrations for a single drug alone that inhibits x% of cell growth. When 50% of cell growth was inhibited ( $x = 50$ ), CI<sub>50</sub> values were achieved according to the IC<sub>50</sub> of the formulas. CI values less than 1 demonstrate the synergism of drug combinations.

### In vivo antitumor efficacy and systemic toxicity

CRC xenograft mice were used to evaluate the *in vivo* antitumor efficacy when tumors reached around 100 mm<sup>3</sup> in volume and were randomly divided into 8 groups (6 mice each group) (Liu et al., 2017). Blank NLC, C I-p/Q NLC, I-p/Q NLC, I-p NLC, I NLC, Q NLC, free I/Q, and 0.9% saline were intravenously injected to the tail vein of mice every three days at an equivalent dose of irinotecan (2 mg/kg) and/or quercetin (2 mg/kg). Tumor length and width were measured with calipers, and the tumor volume ( $V$ ) was calculated as  $V = \text{length} \times \text{width}^2/2$ . The photos of the changes in solid tumors after drug injection were recorded. *In vivo* biosafety was evaluated by the changes in the body weights of mice and other indicators including the creatinine (CRE, the function of kidneys), the alanine aminotransferase (ALT, the function of liver), and the white blood cells (WBC).

### Statistical analysis

Data are presented as means  $\pm$  standard deviation (SD). Statistical analysis was performed by Student's *t*-test (between two groups) or one-way analysis of variance (ANOVA) (among three or more groups). \* $P < .05$  was considered statistically significant.

## Results

### Characterization of I-p

LC-MS of I-p (ES<sup>+</sup>):  $m/z$  calculated for C<sub>46</sub>H<sub>65</sub>N<sub>3</sub>O<sub>7</sub>S<sub>2</sub>: [M + H]<sup>+</sup> 836.4319, found 836.1588. <sup>1</sup>H NMR (600 MHz, DMSO-d<sub>6</sub>) (Figure 1(B)):  $\delta$  0.81, 1.21 belong to SA;  $\delta$  1.87, 4.43, 4.76, 6.92 and 7.39 belong to irinotecan.  $\delta$  2.07, 3.57 prove the formation of amido acid.  $\delta$  2.83 demonstrated the ester bond.

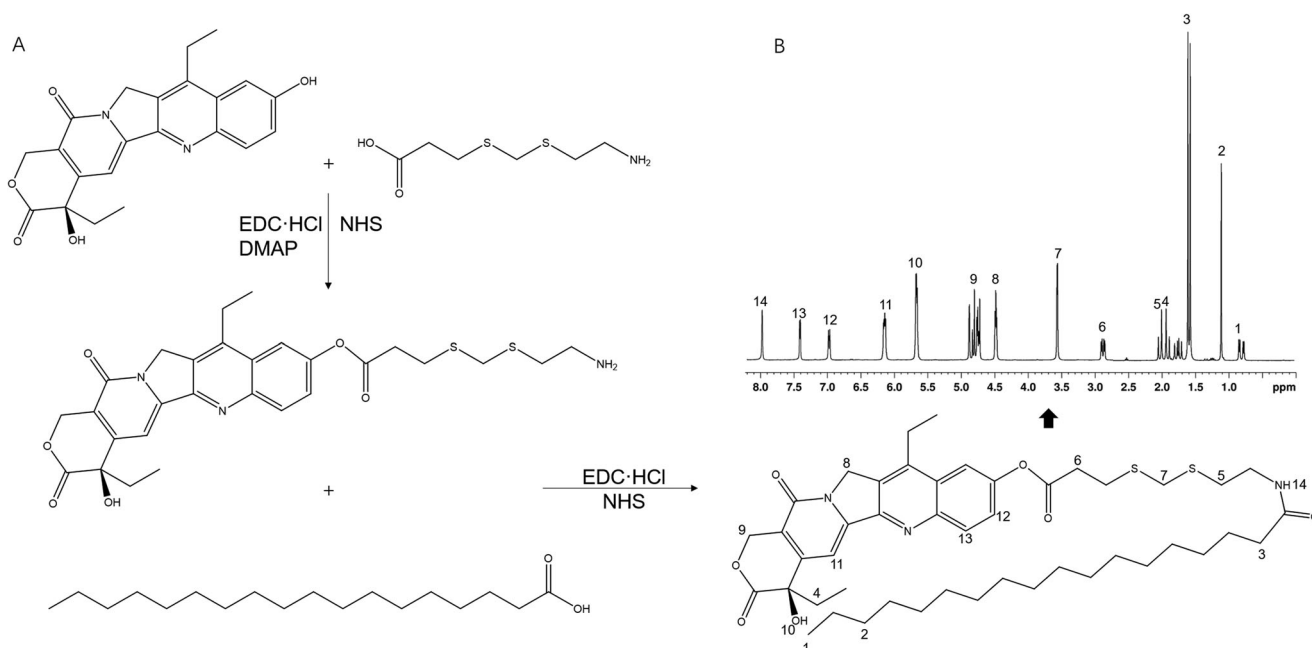


**Figure 1.** Synthesize of an irinotecan prodrug (A) and <sup>1</sup>H NMR (B).

**Table 1.** The mean particle size, size distribution, zeta potential, and drug loading efficiency of NLC.

NLC	Particle size (nm)	Size distribution	Zeta potential (mV)	Drug loading efficiency (%)	
				Irinotecan	Quercetin
C I-p/Q NLC	148.9 ± 4.3	0.17 ± 0.02	-15.6 ± 1.9	85.6 ± 3.9	84.1 ± 3.5
Blank NLC	115.3 ± 3.1	0.14 ± 0.03	-21.3 ± 2.9	/	/
I-p/Q NLC	119.5 ± 4.2	0.16 ± 0.03	-20.1 ± 2.1	84.8 ± 3.7	81.6 ± 3.4
I-p NLC	121.3 ± 3.3	0.12 ± 0.02	-19.3 ± 2.6	82.1 ± 3.3	/
I NLC	120.3 ± 3.2	0.13 ± 0.02	-22.5 ± 1.9	83.9 ± 3.5	/
Q NLC	116.8 ± 3.5	0.15 ± 0.03	-23.5 ± 2.3	/	83.2 ± 3.6

### Characterization of NLC

The particle size, size distribution, zeta potential, and drug loading efficiency of NLC were summarized in Table 1. Figure 2(A) presented the spherical and uniform morphology of blank NLC and C I-p/Q NLC. NLC formulations showed about 120–150 nm in diameter and the size showed no drastic increase during the 72 h of incubation with serum (Figure 2(B)), which could prove the stability of NLC in serum with no aggregation occurred for the period of administration. The NLC was also stable without the presence of serum. The absorbance curves of C I-p/Q NLC and free conatumumab (C) were observed after using a microBCA kit at 562 nm: There is one peak during 12 to 17 min for free conatumumab, while two peaks were there for C I-p/Q NLC, one of which is overlapped with the peak of free conatumumab, demonstrating successful linking of conatumumab to NLC.

### In vitro drug release

As shown in Figure 3, sustained-release behaviors were found on NLC formulations, most of which complete their release after 48 h. Drugs released in normoxia (N) or hypoxic (H) conditions were different. In hypoxic release medium, drug release was more sufficient, over 80% of drugs were released after 48–72 h of study. While in normoxia condition,

only about 60% of drug release was achieved. Irinotecan release was slower from C I-p/Q NLC than that of I-p/Q NLC, indicating the sustained manner *in vitro* to prolong the effect directly.

### Cellular uptake

Figure 4 illustrated the fluorescence images and flow cytometer results. Quantitative data showed that NLC formulations achieved over 60% of uptake when administrated on HT-29 cells. C I-p/Q NLC illustrates 73.2% of cell uptake, which was higher compared with non-decorated NLC formulations.

### Synergistic cytotoxicity

The combination index (CI) vs fraction of the affected cells (Fa) is plotted with different molar ratios of drugs (Figure 5(A)). CI values below 1 were found at molar ratios of 1:1, 2:1, and 4:1 (irinotecan: quercetin, w/w), indicating the synergy of the two drugs at these ratios when co-loaded in NLC formulations. The ratio of 1:1 showed the minimum CI value and was chosen as the amount for the NLC preparation. Cell viability of NLC was evaluated at various drug concentrations using MTT assay. Blank NLC was nontoxic to HT-29 cells, while drugs loaded NLC and free drugs formulas exhibited

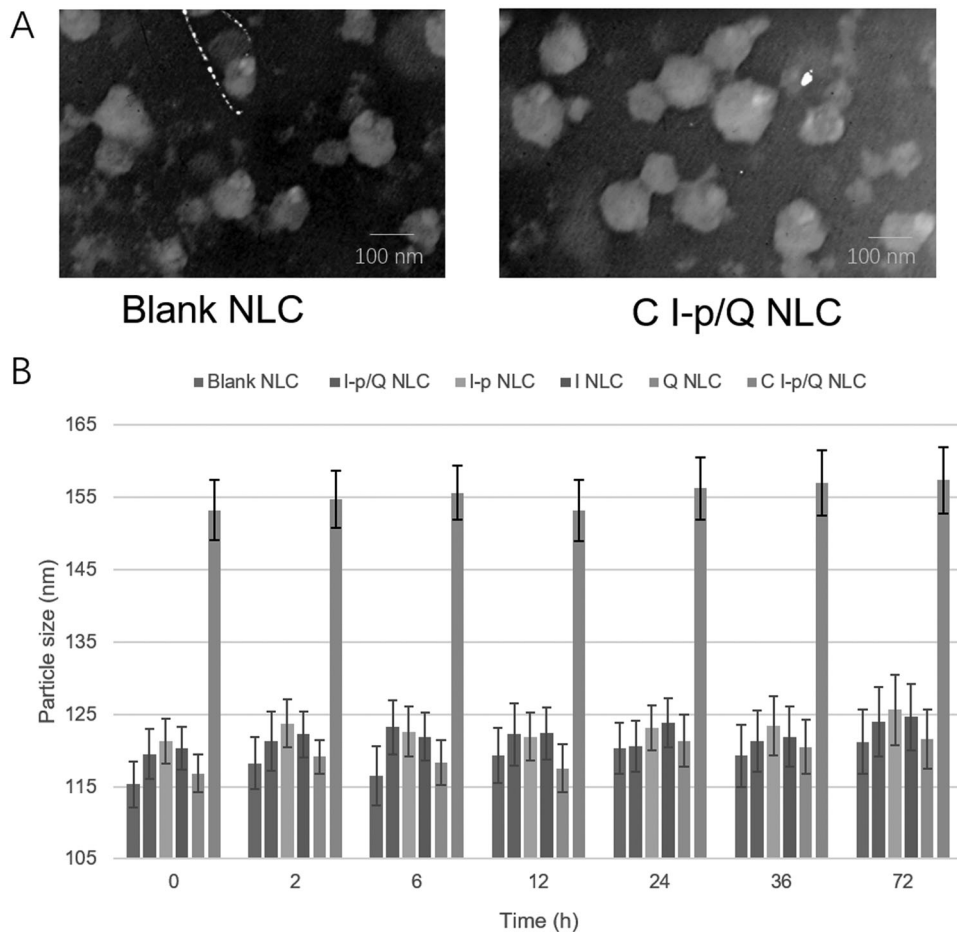


**Figure 2.** The morphology of C I-p/Q NLC (A) and the serum stability of NLC formulations (B).

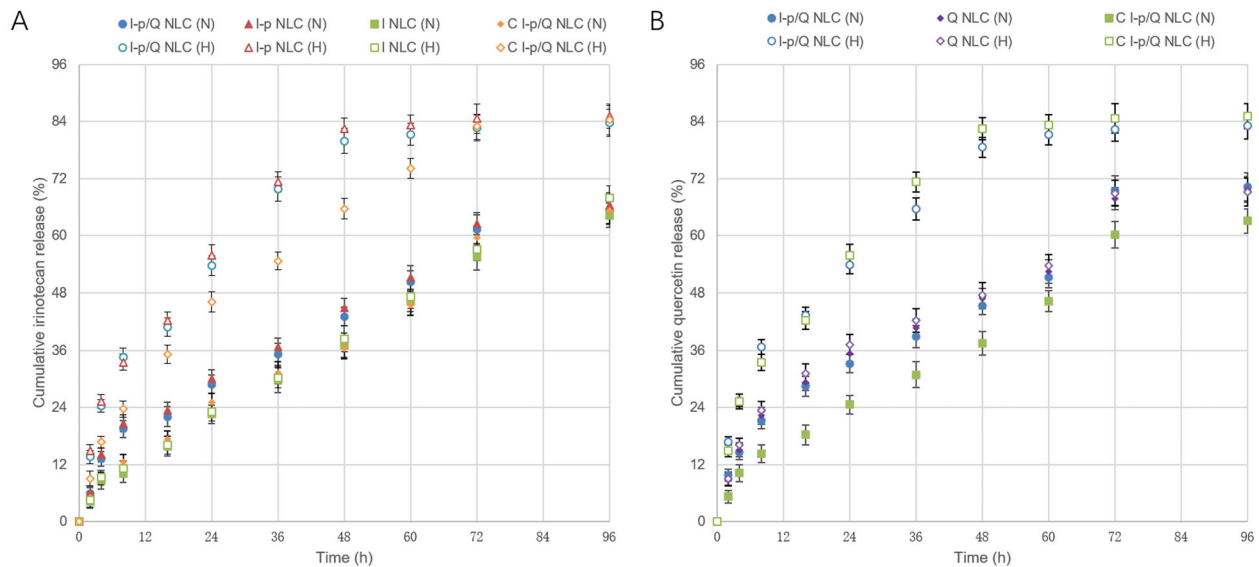


**Figure 3.** *In vitro* irinotecan (A) and quercetin (B) release from NLC. Data presented as means  $\pm$  SD ( $n = 3$ ).

dose-dependent cytotoxicity (Figure 5(B)). C I-p/Q NLC inhibited tumor cells more efficiently than non-decorated I-p/Q NLC ( $P < .05$ ). I-p/Q NLC showed significantly higher cytotoxicity than I-p NLC and Q NLC ( $P < .05$ ), which may attribute to the synergistic effect of two drugs co-loaded in NLC. I-p

NLC exhibited better cell inhibition ability than that of I NLC ( $P < .05$ ), which could prove the efficiency of irinotecan pro-drug. Cell viability of drugs loaded NLC and free drugs formulas exhibited showed no remarkable difference on normal NCM460 cells (Figure 5(C)).



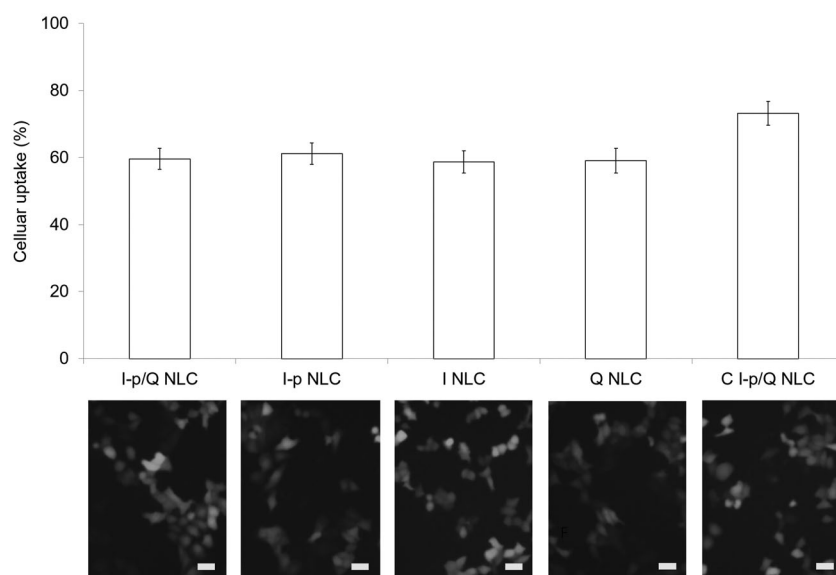


**Figure 4.** Cellular uptake of NLCs: fluorescence images and flow cytometer results. Bars equal to 50  $\mu\text{m}$ . Data presented as means  $\pm$  SD ( $n = 6$ ).

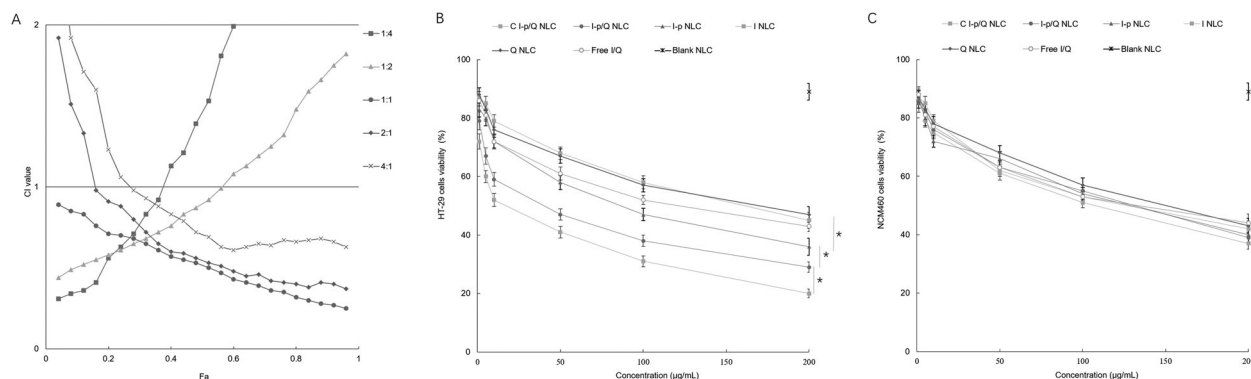


**Figure 5.** The combination index (CI) vs fraction of the affected cells (Fa) (A). Cytotoxic effects were evaluated on HT-29 cells (B) and NCM460 cells (C) by MTT assay. Data presented as means  $\pm$  SD ( $n = 6$ ). \* $P < .05$ .

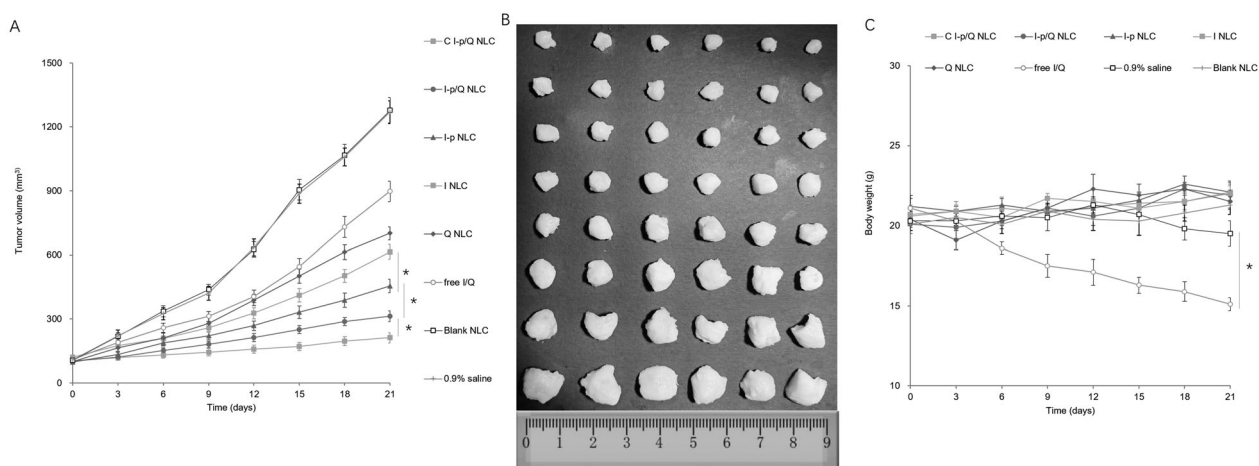


**Figure 6.** *In vivo* tumor growth inhibition efficiency: tumor volume curves (A), tumor images after treatment (B), and body weight lost (C). Data presented as means  $\pm$  SD ( $n = 10$ ). \* $P < .05$ .

***In vivo* antitumor efficacy and systemic toxicity**

C I-p/Q NLC showed the most significant *in vivo* tumor inhibition ability (Figure 6(A)), which was higher than other NLC, free drugs and saline control groups ( $P < .05$ ). I-p/Q NLC also

exhibited higher tumor inhibition efficiency than single drug-loaded NLC ( $P < .05$ ), this may attribute to the synergy effects of the drugs. The photos of the solid tumors before and after drug injection were presented in Figure 6(B). Due to the

obvious better antitumor efficacy of I-p NLC compared with I NLC ( $P < .05$ ), the efficacy of prodrug could be proved. The CRE, ALT and WBC values of both nanoparticles and free drugs are not obviously changed, ensuring biosafety *in vivo*. All of the NLC groups presented no significant change of body weight (Figure 6(C)), while free I/Q treated mice exhibited statistically lower body weights compared to NLC treated mice ( $p < .05$ ), which may indicate the systemic toxicity of the drugs not encapsulated in the NLC.

## Discussion

Nanoparticles are reported to offer high drug loading capacity, sustained drug release, minimal toxicity, and flexibility in the route of administration (Hong et al., 2019). Various kinds of NLCs have been used as drug delivery systems, however, the use of irinotecan prodrug combined with quercetin is firstly reported and showed some novelty in colorectal cancer therapy. Nanoparticulate drug delivery systems exhibiting an average size between 10 and 200 nm tend to represent an optimal range for leveraging the enhanced permeability and retention (EPR) effect and minimizing clearance (Guo & Huang, 2014). The sizes around 120–150 nm in this research are suitable for drug delivery to cancers. The NLC formulations showed a negative surface charge, which could be due to the presence of the anionic materials used in the preparation process. The PDI of each formulation was lower than 0.2, indicating the homogeneous nature of the formulation (Tan & Wang, 2018). Prodrug strategy was applied along with nanotechnology and gained remarkable anticancer efficiency by researchers (Noh et al., 2015; Zhang et al., 2017). So in this study, irinotecan prodrug (I-p) was synthesized and co-loaded into NLC along with quercetin to combine the advantages of these two strategies.

Nanoparticles' stability against physiological conditions is a prerequisite for further application *in vivo*, so 50% FBS was employed to mimic the *in vivo* situation. All the NLC samples exhibited no obvious changes in the hydrodynamic size after mixing with serum media. This may contribute to the maintenance of colloidal stability even in serum-included media (Wang et al., 2018). A distinct advantage offered by a nano-sized drug delivery system is the controlled release of the drug, which greatly intensifies the bioavailability of the drug and lessens the resultant side effects of the drug to healthy body tissues by the EPR effects (Tan & Wang, 2018). A dialysis method was used in the incubation medium to evaluate the release kinetics of drugs from the NLC. Sustained-release behaviors were found on NLC formulations, most of which complete their release after 48 h. Irinotecan release was slower from I-p loaded NLC than that of I NLC, indicating the more sustained manner of the prodrug contained NLC formulas.

Cellular uptake study could provide some circumstantial evidence to display the advantages of the nanoparticle formulation to enter the cancer cells (Duan & Liu, 2018). The improved uptake ability may better penetrate and deliver drugs delivered to improve the efficacy of the standard drug dose, attenuate side effects, and overcome drug resistance.

In this section, over 70% of cell uptake was achieved by C I-p/Q NLC, and around 60% by other NLC formulations when evaluated on HT-29 cells, proving the good uptake efficiency of NLC.

Cell viability assays showed no significant cytotoxicity of blank NLC, which may be proof of the low toxicity of the materials used in the preparation (Wu et al., 2020). Chen et al reported a nanoparticle system and performed more efficient efficiency compared with free drugs on cancer cells (Chen et al., 2016). They concluded that lipid nanoparticles might have the enhanced ability to adhere to the cell membrane due to the similar nature of the lipids and the cell membrane and may enhance the intracellular drug accumulation and perform better in cancer therapy. Dong and colleagues also argued that lipid nanoparticles could protect the drug better until it is internalized by cancer cells, the drugs released from the particles and continuously accumulated within the tumor cells and kill the cancer cells (Dong et al., 2016). It was reported that quercetin in combination with other anticancer drugs exhibits the anticancer activities of the compound and inhibits the expression of the P-gp transporter (Liu et al., 2017). Different drug doses and proportions loaded in one system may have different effects, some of which have a synergistic effect, while others have an antagonistic effect (Chou, 2010). CI was calculated to validate the synergistic effect of drugs co-loaded NLC. The low CI value in this study could be evidence of the nano-system against prior reported systems.

*In vivo* anti-tumor efficiency of drugs loaded NLC exhibited profound efficiency than free drugs, which could be explained by the high structural integrity, high biocompatibility and bioavailability and controlled release capability attributed to the lipid structure of NLC (Nan, 2019). The lipid shell of the system is biocompatible and exhibits behavior similar to that of cell membranes, letting the fusion of the particles to the cell surface and drugs could be delivered more efficiently into the tumor cells (Mandal et al., 2013). *In vivo* antitumor efficiency study revealed that the higher anti-tumor efficiency of C I-p/Q NLC compared with non-decorated I-p/Q NLC, which is in line with the research of Li et al. (2017) They prepared transferrin decorated nanoparticles and argued that the targeted ability of ligand may bring more tumor inhibition effect to the system, thus displayed sufficient suppression of tumor growth. Taking the lower toxicity of NLC formulations due to the negligible body weight lost together, the NLC system exhibited improved anticancer activity along with lower toxicity than the free drugs. The prodrug contained combination nano-system is a promising platform for CRC therapy.

## Conclusion

This developed an I-p/Q NLC for CRC treatment. The results showed that the HT-29 cells uptake of NLC was around 70%. I-p/Q NLC showed significantly higher cytotoxicity than single drug-loaded NLC and free drugs. *In vivo* studies in a CRC-bearing model corroborated the capability of nanoparticles for the inhibition of cancer, leading to a reduction of tumor

growth without systemic toxicity. The prodrug contained combination nano-system is a promising platform for CRC therapy.

## Disclosure statement

The authors do not have any conflict of interest to declare.

## Funding

The author(s) reported there is no funding associated with the work featured in this article.

## References

- Alberts SR, Horvath WL, Sternfeld WC, et al. (2005). Oxaliplatin, fluorouracil, and leucovorin for patients with unresectable liver-only metastases from colorectal cancer: a North Central Cancer Treatment Group phase II study. *J Clin Oncol* 23:9243–9.
- Arnold M, Sierra MS, Laversanne M, et al. (2017). Global patterns and trends in colorectal cancer incidence and mortality. *Gut* 66:683–91.
- Bavi P, Prabhakaran SE, Abubaker J, et al. (2010). Prognostic significance of TRAIL death receptors in Middle Eastern colorectal carcinomas and their correlation to oncogenic KRAS alterations. *Mol Cancer* 9:203.
- Chen W, Guo M, Wang S. (2016). Anti prostate cancer using PEGylated bombesin containing, cabazitaxel loading nano-sized drug delivery system. *Drug Dev Ind Pharm* 42:1968–76.
- Chou TC, Talalay P. (1984). Quantitative analysis of dose-effect relationships: the combined effects of multiple drugs or enzyme inhibitors. *Adv Enzyme Regul* 22:27–55.
- Chou TC. (2010). Drug combination studies and their synergy quantification using the Chou-Talalay method. *Cancer Res* 70:440–6.
- Dong S, Zhou X, Yang J. (2016). TAT modified and lipid – PEI hybrid nanoparticles for co-delivery of docetaxel and pDNA. *Biomed Pharmacother* 84:954–61.
- Duan W, Liu Y. (2018). Targeted and synergistic therapy for hepatocellular carcinoma: monosaccharide modified lipid nanoparticles for the co-delivery of doxorubicin and sorafenib. *Drug Des Devel Ther* 12: 2149–61.
- Falcone A, Ricci S, Brunetti I, et al. (2007). Gruppo Oncologico Nord Ovest. Phase III trial of infusional fluorouracil, leucovorin, oxaliplatin, and irinotecan (FOLFOXIRI) compared with infusional fluorouracil, leucovorin, and irinotecan (FOLFIRI) as first-line treatment for metastatic colorectal cancer: the Gruppo Oncologico Nord Ovest. *JCO* 25:1670–6.
- Fang T, Dong Y, Zhang X, et al. (2016). Integrating a novel SN38 prodrug into the PEGylated liposomal system as a robust platform for efficient cancer therapy in solid tumors. *Int J Pharm* 512:39–48.
- Guo S, Huang L. (2014). Nanoparticles containing insoluble drug for cancer therapy. *Biotechnol Adv* 32:778–88.
- Hong Y, Che S, Hui B, et al. (2019). Lung cancer therapy using doxorubicin and curcumin combination: targeted prodrug based, pH sensitive nanomedicine. *Biomed Pharmacother* 112:108614.
- Li F, Mei H, Gao Y, et al. (2017). Co-delivery of oxygen and erlotinib by aptamer-modified liposomal complexes to reverse hypoxia-induced drug resistance in lung cancer. *Biomaterials* 145:56–71.
- Li S, Wang L, Li N, et al. (2017). Combination lung cancer chemotherapy: design of a pH-sensitive transferrin-PEG-Hz-lipid conjugate for the co-delivery of docetaxel and baicalin. *Biomed Pharmacother* 95:548–55.
- Ling X, Zhang S, Shao P, et al. (2015). Synthesis of a reactive oxygen species responsive heterobifunctional thioether linker. *Tetrahedron Lett* 56:5242–4.
- Liu B, Han L, Liu J, et al. (2017). Co-delivery of paclitaxel and TOS-cisplatin via TAT-targeted solid lipid nanoparticles with synergistic anti-tumor activity against cervical cancer. *Int J Nanomedicine* 12:955–68.
- Liu K, Chen W, Yang T, et al. (2017). Paclitaxel and quercetin nanoparticles co-loaded in microspheres to prolong retention time for pulmonary drug delivery. *Int J Nanomedicine* 12:8239–55.
- Lucas AS, O'Neil BH, Goldberg RM. (2011). A decade of advances in cytotoxic chemotherapy for metastatic colorectal cancer. *Clin Colorectal Cancer* 10:238–44.
- Lv L, Liu C, Chen C, et al. (2016). Quercetin and doxorubicin co-encapsulated biotin receptor-targeting nanoparticles for minimizing drug resistance in breast cancer. *Oncotarget* 7:32184–99.
- Mandal B, Bhattacharjee H, Mittal N, et al. (2013). Core-shell-type lipid-polymer hybrid nanoparticles as a drug delivery platform. *Nanomedicine* 9:474–91.
- Masi G, Vasile E, Loupakis F, et al. (2008). Triplet combination of fluoropyrimidines, oxaliplatin, and irinotecan in the first-line treatment of metastatic colorectal cancer. *Clin Colorectal Cancer* 7:7–14.
- Mathijssen RH, van Alphen RJ, Verweij J, et al. (2001). Clinical pharmacokinetics and metabolism of irinotecan (CPT-11). *Clin Cancer Res* 7: 2182–94.
- Nan Y. (2019). Lung carcinoma therapy using epidermal growth factor receptor-targeted lipid polymeric nanoparticles co-loaded with cisplatin and doxorubicin. *Oncol Rep* 42:2087–96.
- Noh I, Kim HO, Choi J, et al. (2015). Co-delivery of paclitaxel and gemcitabine via CD44-targeting nanocarriers as a prodrug with synergistic antitumor activity against human biliary cancer. *Biomaterials* 53: 763–74.
- Rashedi J, Ghorbani Haghjo A, Mesgari Abbasi M, et al. (2019). Anti-tumor effect of quercetin loaded chitosan nanoparticles on induced colon cancer in Wistar rats. *Adv Pharm Bull* 9:409–15.
- Roese E, Bunjes H. (2017). Drug release studies from lipid nanoparticles in physiological media by a new DSC method. *J Control Release* 256: 92–100.
- Ruan C, Liu L, Lu Y, et al. (2018). Substance P-modified human serum albumin nanoparticles loaded with paclitaxel for targeted therapy of glioma. *Acta Pharm Sin B* 8:85–96.
- Shao Z, Shao J, Tan B, et al. (2015). Targeted lung cancer therapy: preparation and optimization of transferrin-decorated nanostructured lipid carriers as novel nanomedicine for co-delivery of anticancer drugs and DNA. *Int J Nanomedicine* 10:1223–33.
- Slatter JG, Su P, Sams JP, et al. (1997). Bioactivation of the anticancer agent CPT-11 to SN-38 by human hepatic microsomal carboxylesterases and the in vitro assessment of potential drug interactions. *Drug Metab Dispos* 25:1157–64.
- Tan S, Wang G. (2018). Lung cancer targeted therapy: folate and transferrin dual targeted, glutathione responsive nanocarriers for the delivery of cisplatin. *Biomed Pharmacother* 102:55–63.
- Tiernan JP, Perry SL, Verghese ET, et al. (2013). Carcinoembryonic antigen is the preferred biomarker for in vivo colorectal cancer targeting. *Br J Cancer* 108:662–7.
- Van Cutsem E, Nordlinger B, Adam R, et al. (2006). Towards a pan-European consensus on the treatment of patients with colorectal liver metastases. *Eur J Cancer* 42:2212–21.
- Wang J, Sun X, Mao W, et al. (2013). Tumor redox heterogeneity-responsive prodrug nanocapsules for cancer chemotherapy. *Adv Mater* 25: 3670–6.
- Wang Z, Wei Y, Fang G, et al. (2018). Colorectal cancer combination therapy using drug and gene co-delivered, targeted poly(ethylene glycol)- $\epsilon$ -poly(caprolactone) nanocarriers. *Drug Des Devel Ther* 12:3171–80.
- Wang Z, Zang A, Wei Y, et al. (2020). Hyaluronic acid capped, irinotecan and gene co-loaded lipid-polymer hybrid nanocarrier-based combination therapy platform for colorectal cancer. *Drug Des Devel Ther* 14: 1095–105.
- Wang CH, Yoo E, Hur SK, et al. (2018). A highly GSH-sensitive SN-38 prodrug with an "OFF-to-ON" fluorescence switch as a bifunctional anticancer agent. *Chem Commun* 54:9031–4.
- Wu R, Zhang Z, Wang B, et al. (2020). Combination chemotherapy of lung cancer - co-delivery of docetaxel prodrug and cisplatin using aptamer-decorated lipid-polymer hybrid nanoparticles. *Drug Des Devel Ther* 14:2249–61. Jun 9
- Xing J, Zhang X, Wang Z, et al. (2019). Novel lipophilic SN38 prodrug forming stable liposomes for colorectal carcinoma therapy. *Int J Nanomedicine* 14:5201–13.



- Xu G, Shi H, Ren L, et al. (2015). Enhancing the anti-colon cancer activity of quercetin by self-assembled micelles. *Int J Nanomedicine* 10: 2051–63.
- Yang G, Wu F, Chen M, et al. (2019). Formulation design, characterization, and in vitro and in vivo evaluation of nanostructured lipid carriers containing a bile salt for oral delivery of gypenosides. *Int J Nanomedicine* 14:2267–80.
- Yarjanli Z, Ghaedi K, Esmaeili A, et al. (2019). The antitoxic effects of quercetin and quercetin-conjugated iron oxide nanoparticles (QNPs) against H<sub>2</sub>O<sub>2</sub>-induced toxicity in PC12 cells. *Int J Nanomedicine* 14: 6813–30.
- Yuan M, Qiu Y, Zhang L, et al. (2016). Targeted delivery of transferrin and TAT co-modified liposomes encapsulating both paclitaxel and doxorubicin for melanoma. *Drug Deliv* 23:1171–83.
- Zhang J, Shen L, Li X, et al. (2019). Nanoformulated codelivery of quercetin and alantolactone promotes an antitumor response through synergistic immunogenic cell death for microsatellite-stable colorectal cancer. *ACS Nano* 13:12511–24.
- Zhang J, Xiao X, Zhu J, et al. (2018). Lactoferrin- and RGD-comodified, temozolomide and vincristine-co-loaded nanostructured lipid carriers for gliomatosis cerebri combination therapy. *Int J Nanomedicine* 13: 3039–51.
- Zhang R, Ru Y, Gao Y, et al. (2017). Layer-by-layer nanoparticles co-loading gemcitabine and platinum (IV) prodrugs for synergistic combination therapy of lung cancer. *Drug Des Devel Ther* 11:2631–42.
- Zhang S, Wang J, Pan J. (2016). Baicalin-loaded PEGylated lipid nanoparticles: characterization, pharmacokinetics, and protective effects on acute myocardial ischemia in rats. *Drug Deliv* 23:3696–703.
- Zhu B, Yu L, Yue Q. (2017). Co-delivery of vincristine and quercetin by nanocarriers for lymphoma combination chemotherapy. *Biomed Pharmacother* 91:287–94.